

Impeded Growth of Magnetic Flux Bubbles in the Intermediate State Pattern of Type I Superconductors

V. Jeudy and C. Gourdon

*Groupe de Physique des Solides, Universités Paris 6 et 7, CNRS UMR 75-88, Campus Boucicaut,
140 rue de Lourmel, 75014 Paris, France*

T. Okada

*Itoh Laboratory, Division of Materials Physics, School of Engineering Science, Osaka University,
1-3 Machikaneyama-cho, Toyonaka-shi, Osaka 560-8531, Japan*

(Received 2 September 2003; published 6 April 2004)

Normal state bubble patterns in type I superconducting indium and lead slabs are studied by the high resolution magneto-optical imaging technique. The size of bubbles is found to be independent of the long-range interaction between the normal state domains. Under bubble diameter and slab thickness proper scaling, the results gather onto a single master curve. We calculate the equilibrium diameter of an isolated bubble resulting from the competition between the Biot-and-Savart interaction of the Meissner current encircling the bubble and the superconductor-normal interface energy. A good quantitative agreement with the master curve is found over two decades of the magnetic Bond number. The isolation of each bubble in the superconductor and the interface energy are shown to preclude any continuous size variation of the bubbles after their formation, contrary to the prediction of mean-field models.

DOI: 10.1103/PhysRevLett.92.147001

PACS numbers: 74.25.Ha, 05.65.+b, 75.70.Kw

A great variety of quasi-two-dimensional, biphasic systems presents a spontaneous formation of domain patterns: magnetic liquids [1], Langmuir monolayers [2], submonolayer of adsorbed atoms [3], ferro- and ferrimagnetic films [4], intermediate state (IS) in type I superconducting (SC) materials [5]. These structures are mostly interpreted as resulting from the balance between long-range repulsive, electrostatic, magnetic, or elastic interactions between domains and short-range attractive interaction associated with a positive interface energy. The observed patterns are generally disordered and consist of bubbles and of branched and intricate fingered structures (lamellae). At present the mechanisms of the formation of these structures are theoretically actively studied [6–8]. In particular, for magnetic fluids, the instabilities of bubble circular shape was shown to produce fingered structures which are similar to those observed experimentally [6]. The same mechanism was proposed for the IS in type I superconductors [9]. However, little is known even about the static properties of bubble patterns [10]. This question is of prime importance for the study of IS patterns formation since normal state (NS) bubbles form the early stage of the IS when the magnetic flux starts to penetrate into SC samples [5].

IS patterns are observed in slabs placed in a perpendicular magnetic field. They consist of SC and NS, flux-bearing domains [5]. Former studies were essentially focused on the lamella structures [5]. The free energy of a one-dimensional lattice of infinitely long and parallel stripes was first calculated by Landau [11]. The field-dependent predicted and measured periods of the stripes were found in good agreement [12]. Subsequently, their comparison became a conventional method for determin-

ing the interface energy of type I SC materials. The formation of lamellae was recently reexamined by Dorsey *et al.* and in the framework of a “current-loop” model [9]. These authors propose to consider IS patterns as a set of domains of arbitrary shapes with vertical domain walls and bounded by current loops interacting in the free space above and below the slabs [9]. When applied to the stripe pattern the model predicts equilibrium periods close to those found using the Landau model, thus indicating that both models essentially capture the same physics. As the model is formulated for arbitrary domain shape, it opens the way to study the formation of bubble patterns whose conditions of existence and control parameters are not well understood. To our knowledge, the only calculation of the free energy of a hexagonal lattice of bubbles uses an approximate expression of the magnetic interaction energy [13]. Subsequent experiments found a field-dependent bubble spacing different from the predicted one. They also yield a smaller interfacial tension than the one deduced from the studies of stripe patterns [13–16]. In view of these scarce and contradictory results, it cannot be established whether bubble patterns correspond to a quasiground state as is the case for stripe patterns. Furthermore, the onset of the formation of the IS was shown to result from the penetration of bubbles from the edges of samples [17]. The magnetic flux penetration is controlled by an energy barrier of geometrical nature [18,19]. This raises the question of the respective contributions of the mechanism of flux penetration and of the balance between long-range and short-range interactions on the formation of bubble patterns.

This Letter presents a systematic study of NS bubble patterns as a function of the SC material, the slab

thickness, and the applied magnetic field. Contrary to the lamellae width, the diameter of the bubbles is found to be independent of the mutual interaction between flux-bearing domains. We discuss the origin of these different behaviors in terms of magnetic flux penetration mechanisms.

The domain patterns are observed with the high resolution Faraday microscopy technique which probes the normal component of the local induction at the top surface of a superconductor. Experimental details are given elsewhere [20]. The SC Pb slabs were cut out from Good-Fellow 99.9% pure and annealed 25 and $120 \pm 1 \mu\text{m}$ thick foils. The magneto-optic layer (MOL) consisted of a 1500 \AA EuS film evaporated on a glass substrate and covered with a 600 \AA Al mirror. The Pb slab was compressed against the mirror. The In slabs ($0.6, 1.1, 1.5, 2.2, 10.0 \pm 0.1 \mu\text{m}$ thick) were obtained by evaporation directly onto MOLs. The MOLs consisted of CdMnTe/CdMgTe semiconductor heterostructures grown by molecular beam epitaxy [21]. The samples were immersed into superfluid helium at temperatures $T \leq 2 \text{ K}$. They were subjected to an increasing perpendicular magnetic field H whose maximum value equals 60 mT .

Figure 1 shows typical IS patterns observed on the edge of a $10 \mu\text{m}$ thick indium slab for two values of the reduced applied magnetic field $h = H/H_c$, where H_c is the thermodynamical critical field. Increasing h results in the penetration of the magnetic flux from the edges of the slab which is revealed by a significant increase of the density of NS domains. At low h value (left image), NS domains essentially consist of almost circular bubbles. They were systematically observed over a limited range of low h values. At higher h value (right image), lamellae have appeared. They progressively form labyrinthine structures.

While most of the lamellae are connected to the slab edges from which the magnetic flux enters, bubbles are isolated in the SC matrix and separated from the edges by a full diamagnetic band ($\approx 50 \mu\text{m}$ large). Let us note that (i) the interaction between isolated NS domains is repul-

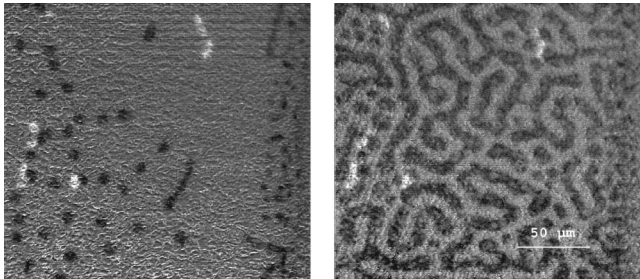


FIG. 1. Intermediate state pattern on the edge of the $10 \mu\text{m}$ thick superconducting indium slab for $h = 0.07$ (left) and $h = 0.41$ (right) at $T = 2 \text{ K}$. The edge of the In slab is along the right edge of the images. Normal and superconducting domains appear in black and gray, respectively. The few white domains correspond to magnetic flux which was trapped at $h = 0$ (details on image processing are given in Ref. [20]).

sive and (ii) the diamagnetic band reflects the presence of the geometrical energy barrier that prevents spontaneous flux penetration on the edges [18,19]. Therefore different formation and growth mechanisms are expected for bubbles and lamellae.

In order to get more insight into this question, the variation of the bubble diameter $2R$ and the lamella width W were measured systematically as a function of h . They were then compared to their respective equilibrium values $2R_{\text{eq}}$ and W_{eq} , calculated for regular arrays. Figure 2 presents the results obtained for a $10 \mu\text{m}$ thick In slab (left) and for a $120 \mu\text{m}$ thick Pb slab (right). For the lamella pattern, W_{eq} is calculated from Eqs. (3.23) and (4.8) of Ref. [9]. For the bubble pattern, R_{eq} is calculated in the framework of the current-loop model [9]. NS bubbles with radii R are assumed to be arranged in a hexagonal lattice of period a in an infinite slab of thickness d . The magnetic field in the bubbles is equal to H_c [9]. From the constraint of global flux conservation the area fraction of NS domains $\rho_n = 2\pi R^2/\sqrt{3}a^2$ is equal to $h = H/H_c$. The interface energy E_{int} is the product of the interfacial tension $\sigma_{ns} = (H_c^2/8\pi)\Delta$ by the total area of the interfaces $2N\pi R d$, where N and Δ are the total number of bubbles and the “wall” energy parameter, respectively. The magnetic energy per unit area resulting from the self- and mutual interaction between the screening currents flowing at the interfaces is found equal to

$$\epsilon_m = -\frac{y^2 N_b}{3\pi} \sum_{m=-\infty}^{+\infty} \sum_{t=-\infty}^{+\infty} \frac{J_1^2(y_s)}{s^2} \left(1 - \frac{1 - \exp(-2\pi ds/a)}{2\pi ds/a} \right), \quad (1)$$

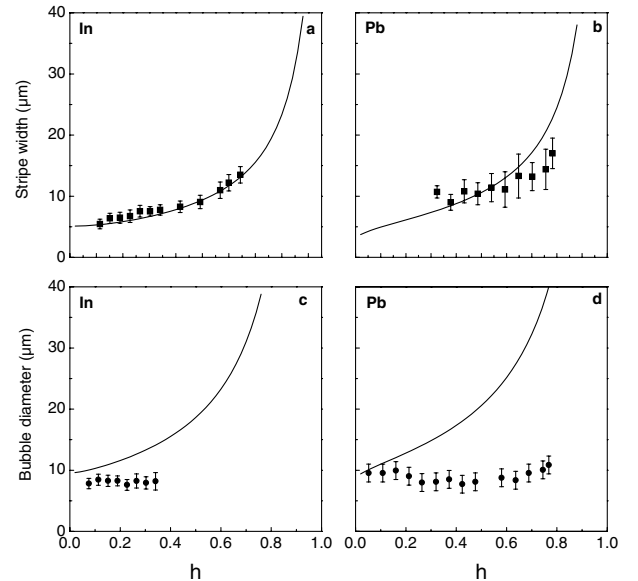


FIG. 2. Mean lamella width W (top) and bubble diameter $2R$ (bottom) as a function of the reduced field $h = H/H_c$ for a $10 \mu\text{m}$ thick In slab (left) and a $120 \mu\text{m}$ thick Pb slab (right). The error bars represent the full width at half maximum of the distributions of lamella width or bubble diameter. The solid lines are the equilibrium values $2R_{\text{eq}}$ and W_{eq} .

with $s = \sqrt{4(m^2 + t^2 - mt)/3}$, $y = \sqrt{2\pi\sqrt{3}\rho_n}$. J_1 is the Bessel function of the first kind, $N_b = d/\pi\Delta$ is the magnetic Bond number [9], and ϵ_m is expressed in units of σ_{ns} . The equilibrium period a_{eq} is obtained by minimizing the reduced total energy per unit area $\epsilon(a) = \epsilon_{\text{int}} + \epsilon_m$. R_{eq} is then obtained from flux conservation as $R_{\text{eq}} = a_{\text{eq}}\sqrt{\sqrt{3}h/2\pi}$. $H_c(T)$ was assumed to follow a Bardeen-Cooper-Schrieffer temperature variation: $H_c(T) = H_c(0)[1 - (T^2/T_c^2)]$. $H_c(0)$ is 28.2 and 80.3 mT and T_c is 3.4 and 7.2 K for indium and lead, respectively. $\Delta(T)$ was assumed to follow the empirical law $\Delta(T) = \Delta(0)/\sqrt{1 - (T/T_c)}$ as proposed in Ref. [22]. $\Delta(0)$ values were taken from the literature: for Pb, $\Delta(0) = 0.056 \mu\text{m}$ [5]; for In, $\Delta(0) = 0.33 \mu\text{m}$ [22].

For the lamellae, W and W_{eq} present a good quantitative agreement, as often reported in the literature [see Figs. 2(a) and 2(b)]. The slight discrepancy obtained for Pb, for $h > 0.65$, may be attributed to the fact that an important fraction of the lamellae remains isolated among bubbles. Surprisingly, the measured bubble diameter $2R$ is found to remain almost constant, as h is increased, in disagreement with the theoretical predictions [see Figs. 2(c) and 2(d)]. The maximum ratio between $2R_{\text{eq}}$ and $2R$ is of the order of 1.6 and 4 for In and Pb, respectively. However, $2R$ approaches $2R_{\text{eq}}$ for $h \rightarrow 0$, thus suggesting that the disagreement does not originate from the approximations used in the model of Ref. [9].

To clarify this point, the bubble diameter $2R$ was measured for different slab thicknesses d and compared to $2R_{\text{eq}}^0$, the limit of $2R_{\text{eq}}$ calculated for $h \rightarrow 0$. In this limit, the magnetic energy is determined only by the self-interaction of the screening currents flowing at each bubble interface. We find that $2R_{\text{eq}}^0$ is the solution of the implicit equation:

$$N_b = \frac{3(1-k^2)}{k^2} \left[1 + \frac{1}{k^3} [(k^2-2)E(k) + 2(1-k^2)K(k)] \right]^{-1}, \quad (2)$$

with $k^2 = 4R_{\text{eq}}^0{}^2/(d^2 + 4R_{\text{eq}}^0{}^2)$. K and E are the complete elliptic integrals of the first and the second kind, respectively. Equation (2) is transformed into a relation between the reduced variables $2R_{\text{eq}}^0/\Delta$ and d/Δ as plotted in Fig. 3. The same figure reports the results obtained by us and by other authors with different SC materials (In, Pb, and Hg) [23]. Scaling $2R$ and d by the wall energy parameter Δ allows one to gather all the measured diameters onto a single master curve. This demonstrates that $2R/\Delta$ and d/Δ are appropriate reduced variables to describe the bubble patterns. Furthermore, the magnetic Bond number $N_b = d/\pi\Delta$ varies over the full range of existence of nonbranching IS patterns ($1 < N_b < 1000$) [13,24]. For smaller Bond numbers the gray region in Fig. 3 indicates the occurrence of type II superconductivity below a critical thickness d_c . Indeed, no IS domains were observed for the thinnest In slab ($d = 0.6 \mu\text{m}$).

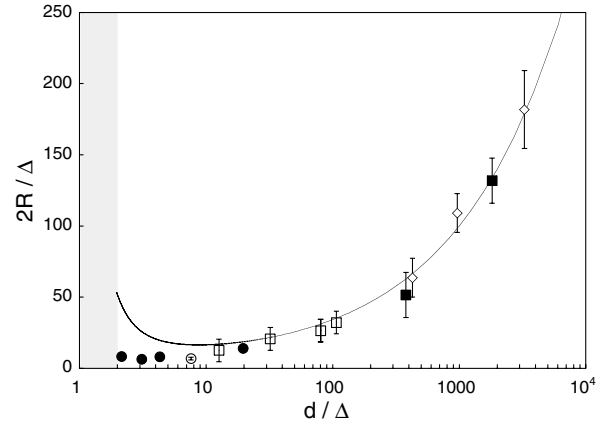


FIG. 3. Semilog plot of the reduced bubble diameter $2R/\Delta$ versus reduced sample thickness d/Δ . The filled circles and squares were obtained with In and Pb slabs, respectively. The empty squares, lozenges, and circles are reported from Refs. [14–16], for Pb, Hg, and In, respectively. The gray region corresponds to type II superconductivity for very thin slabs. The solid curve is the equilibrium diameter [Eq. (2)].

The comparison between the master curve and the prediction of Eq. (2) shows that two ranges of d/Δ values can be distinguished. For $d/\Delta < 30$, $2R$ values are found slightly smaller than $2R_{\text{eq}}$. In this range of thickness, the assumption of a constant Δ is no longer valid. As the thickness decreases towards the critical value d_c the interfacial tension (positive for a type I superconductor and negative for a type II one) should decrease. Indeed adjusting the experimental data to the predicted curve leads to a continuous decrease of Δ with decreasing d (not shown here). The critical thickness at which $\Delta \rightarrow 0$ was found equal to $d_c = 0.8 \mu\text{m}$, a value consistent with $d_c \approx 0.9\text{--}1 \mu\text{m}$ reported for In in Ref. [13]. Therefore, the poor agreement found for $d/\Delta < 30$ most likely originates from the reduction of the interface energy when the slab thickness is decreased. For $d/\Delta > 30$, the master curve presents a very good quantitative agreement with the prediction of Eq. (2). This shows that the bubble mean diameter is determined by the balance between the interfacial tension and the *self*-interaction of the screening current flowing at the bubble interface. While the bubble diameter remains constant when h increases, as shown in Fig. 2, the mutual interaction between the bubbles serves to adjust the mean distance between them so that the area density of NS domains ρ_n is very close to the equilibrium value. We calculate that the bubbles free energy is only $\approx 1\%$ larger than the equilibrium value. The reason is that volume terms depending on ρ_n , but not on the period, are dominant in the free energy. Hence the bubble system is only in a very slightly out-of-equilibrium state.

These results raise the question of the growth mechanisms of NS domains. For the lamellae, the good agreement between the predicted and the measured width suggests that their growth is continuous and reversible, as assumed by the IS models. This most likely results

from the fact that lamellae are connected to the edges of the slab, thus allowing infinitesimal amounts of magnetic flux to penetrate continuously from the exterior. This is not the case when NS domains are isolated within the SC matrix. As the flux density is uniformly equal to zero in the matrix, it follows from the constraint of flux conservation that the increase of the size of an isolated NS bubble has to result from the incoming of another NS bubble crossing the surrounding SC region. The fusion of these two bubbles is impeded by their repulsive interaction. Moreover, surface tension prevents the formation of bubbles of size much smaller than $2R_{\text{eq}}^0$. This precludes the continuous and reversible growth of bubbles. Therefore, they have to keep the size acquired during their formation as it is observed experimentally. A similar phenomenon should be encountered in other physical systems for which the mechanism of growth of isolated domains requires the migration of particles or of flux lines through a second phase. For example, in a ferrofluid confined in a Hele-Shaw cell with an immiscible nonmagnetic liquid, the inhibited migration of magnetic particles between domains should prevent their size variation.

The early stage of bubble formation and migration is not accessible experimentally. Bubble velocities close to the sample edges ($>1 \mu\text{m}/\mu\text{s}$) [17] are beyond our experimentally measurable velocities ($\approx 1 \mu\text{m}/\text{s}$). Therefore, only a qualitative and partial understanding of bubble penetration can be inferred from the results presented above. The concentration of bubbles was observed to increase with h essentially while the diamagnetic band is present (see Fig. 1). The bubbles should therefore be formed in the region of the edges and cross the diamagnetic band to reach the sample interior. The characteristic sizes of the domains observed on the edges are smaller than those observed within the bulk. This suggests that the bubbles have to grow and to come unfastened from the IS structures present on the edges of the slab. The motion of the bubbles towards the center of the slab is driven by the magnetic interaction between the flux-bearing domains and the magnetic field around the slab. However, the size of the bubbles was found to be independent of the aspect ratio of the slabs. This indicates that, even if the magnetic field gradient plays a role in the instability giving birth to a bubble, its size is essentially controlled by the competition between the surface tension and the self-interaction of the screening current. It would be of great interest to determine to what extent the size of the domains observed in other diphasic systems results more from specific mechanisms of the formation of domains than from the competition between long- and short-range interactions.

Experimental evidence of the branching instabilities of circular NS bubbles, as proposed in Ref. [7], was not found. Branched domains always bear a much larger

magnetic flux than bubbles. As a result the branching instabilities of bubbles are unlikely to be the prevalent mechanism for the formation of fingered structures. Whether, as in the case of bubbles, this formation results from an instability of the IS structure located on the edge of the sample remains to be investigated.

The authors thank A.O. Cebers for numerous and fruitful discussions.

-
- [1] F. Elias, C. Flament, J.-C. Bacri, and S. Neveu, *J. Phys. I (France)* **7**, 711 (1997).
 - [2] H. M. McConnell, *Annu. Rev. Phys. Chem.* **42**, 171 (1991).
 - [3] R. Plass, N. C. Bartelt, and G. L. Kellogg, *J. Phys. Condens. Matter* **14**, 4227 (2002).
 - [4] M. Seul and R. Wolfe, *Phys. Rev. A* **46**, 7519 (1992).
 - [5] R. P. Huebener, *Magnetic Flux Structures in Superconductors* (Springer-Verlag, New York, 1979).
 - [6] S. A. Langer, R. E. Goldstein, and D. P. Jackson, *Phys. Rev. A* **46**, 4894 (1992).
 - [7] R. E. Goldstein, D. P. Jackson, and A. T. Dorsey, *Phys. Rev. Lett.* **76**, 3818 (1996).
 - [8] A. Cebers, *Phys. Rev. E* **61**, 700 (2000).
 - [9] A. T. Dorsey and R. E. Goldstein, *Phys. Rev. B* **57**, 3058 (1998).
 - [10] Instead of the terms “flux tubes” or “flux spots” found in the literature dedicated to IS studies, we here adopt the conventional designation used for pattern studies.
 - [11] L. D. Landau, *Sov. Phys. JETP* **7**, 371 (1937).
 - [12] R. E. Miller and G. D. Cody, *Phys. Rev.* **173**, 494 (1968).
 - [13] R. N. Goren and M. Tinkham, *J. Low Temp. Phys.* **5**, 465 (1971).
 - [14] R. P. Huebener, R. T. Kampwirth, and V. A. Rowe, *Cryogenics* **12**, 100 (1972).
 - [15] D. E. Farrell, R. P. Huebener, and R. T. Kampwirth, *J. Low Temp. Phys.* **19**, 99 (1975).
 - [16] R. P. Huebener and R. T. Kampwirth, *Phys. Status Solidi (a)* **13**, 255 (1972).
 - [17] D. E. Chimenti and J. R. Clem, *Philos. Mag. B* **38**, 635 (1978).
 - [18] V. Jeudy, G. Jung, D. Limagne, and G. Waysand, *Physica (Amsterdam)* **225C**, 331 (1994).
 - [19] H. Castro, B. Dutoit, A. Jacquier, M. Baharami, and L. Rinderer, *Phys. Rev. B* **59**, 596 (1999).
 - [20] G. Gourdon, V. Jeudy, M. Menant, D. Roditchev, Le Anh Tu, E. L. Ivchenko, and G. Karczewski, *Appl. Phys. Lett.* **82**, 230 (2003).
 - [21] C. Gourdon, G. Lazard, V. Jeudy, C. Testelin, E. L. Ivchenko, and G. Karczewski, *Solid State Commun.* **123**, 299 (2002).
 - [22] Yu. V. Sharvin, *Zh. Eksp. Teor. Fiz.* **38**, 298 (1960); [*Sov. Phys. JETP* **11**, 216 (1960)].
 - [23] For Hg we take $\Delta(0)$ equal to $0.084 \mu\text{m}$, i.e., 3 times smaller than the value proposed in Ref. [15]. The overestimation of $\Delta(0)$ in Ref. [15] results from the use of an approximate model to calculate the magnetic energy.
 - [24] A. Hubert, *Phys. Status Solidi* **24**, 669 (1967).